Preliminary version of a paper to appear at
Elsevier Ad Hoc Networks Journal

Design and Analysis of a Propagation Delay Tolerant ALOHA Protocol for Underwater Networks

(Technical Report No.: ISI-2010-668)

Joon Ahn[a], Affan Syed[b], Bhaskar Krishnamachari[a], John Heidemann[b]

[a]*Ming Hsieh Department of Electrical Engineering*
University of Southern California, Los Angeles, CA 90089
[b]*Computer Science Department and Information Sciences Institute*
University of Southern California, Los Angeles, CA 90089

Abstract

Acoustic underwater wireless sensor networks (UWSN) have recently gained attention as a topic of research. Such networks are characterized by increased uncertainty in medium access due not only to when data is sent, but also due to significantly different propagation latencies from spatially diverse transmitters—together, we call these *space-time uncertainty*. We find that the throughput of slotted ALOHA degrades to pure ALOHA in such an environment with varying delay. We therefore propose handling this spatial uncertainty by adding guard times to slotted ALOHA, forming Propagation Delay Tolerant (PDT-)ALOHA. We show that PDT-ALOHA increases throughput by 17–100% compared to simple slotted ALOHA in underwater settings. We analyze the protocol's performance both mathematically and via extensive simulations. We find that the throughput capacity decreases as the maximum propagation delay increases, and identify protocol parameter values that realize optimal throughput. Our results suggest that shorter hops improve throughput in UWSNs.

Keywords:
Underwater Acoustic Network, ALOHA protocol, Medium Access Control Protocol, Performance Analysis, Optimization

1. Introduction

Underwater sensor networking (UWSN) is becoming an important area of research [1, 2, 3]. Medium access control (MAC) in underwater networks has attracted strong attention due to its potentially large impact to the overall network performance [4, 5, 6, 7]. The most significant change from traditional radio-frequency (RF) networks to underwater acoustic networks is the change of the *medium*: acoustic instead of RF electromagnetic waves. Latency and bandwidth have significant effects on control algorithms

Email addresses: joonahn@usc.edu (Joon Ahn), asyed@isi.edu (Affan Syed), bkrishna@usc.edu (Bhaskar Krishnamachari), johnh@isi.edu (John Heidemann)

for MAC protocols. Both of these vary substantially in acoustic networks where propagation latencies are five-orders of magnitude greater than RF, while bandwidths are one-thousandth that of RF.

ALOHA protocols have been the basis of many wireless MACs since their invention in the 1970s [8]. They are the first class of contention-based MAC protocols in a shared wireless medium. Later protocols, such as carrier sense multiple access (CSMA), achieve better performance than ALOHA in RF networks, due to their conservative mechanism of "listening before transmitting" [9]. However, carrier sense becomes very expensive in underwater acoustic networks due to the large propagation delay. The effect of the propagation delay on ALOHA protocols has been analyzed by Kleinrock and Tobagi [9] showing that the protocols are not sensitive to the propagation delay. However, their analysis does not consider the varying propagation delays from different locations of nodes; thus its results do not completely hold for underwater networks.

The goal of this paper is to understand the impact of varying propagation latency on medium access, with ALOHA protocols as a case study. First, we show that the location-dependent propagation latency has a fundamental impact on the slotted ALOHA because, intuitively, a packet's receive time at the receiver depends not only on its transmit time (time uncertainty) but also on its relative propagation delay to the receiver (space uncertainty). We refer to this joint uncertainty as *space-time uncertainty*. We show that both dimensions of uncertainty need to be handled at the same time. Then, we propose the Propagation Delay Tolerant ALOHA (PDT-ALOHA) protocol to improve the performance of the slotted ALOHA by adding guard times. We explore its performance through mathematical analysis and extensive simulations with an aim to discover the best operating parameters. We find that, in the high latency environment of UWSN, throughput capacity (*i.e.* throughput optimized across all loads) of PDT-ALOHA improves by 17–100% compared to slotted ALOHA, depending on network propagation delay. Our analysis show that the throughput can be kept within 97% of optimal capacity of PDT-ALOHA with an additional slot time that is 69% of the maximum propagation delay, indicating that even with unknown or variable delay regime a pre-configured value of PDT-ALOHA is a substantial improvement on slotted ALOHA. We also find that the throughput capacity decreases with increased propagation delay, reinforcing the benefit of short-range, multi-hop communication in underwater networks besides simply energy-efficient communication.

This paper combines and extends two previous published results [10, 11]. The first of these prior works focused on protocol simulation [10], and the other on analysis [11]; here we combine these results to both validate each against the other in common scenarios, and to provide a definitive discussion of the conclusions. We therefore integrate related work (Section 2) and align the metrics across the two papers for consistent comparison of experiments (Section 7). We confirm that both simulations and analysis are consistent with each other. Finally in Section 7.4 we present a strong argument based on results from ours and concomitant research that motivates short, multi-hop networks in an underwater acoustic environment

Our work is meant to explore intrinsic characteristics of the high latency acoustic channel in UWSN. Work on more sophisticated protocols than ALOHA is already underway for underwater networks, but we expect the evaluation and understanding

we develop here will support the ongoing development of new protocols.

2. Related Work

Recently there has been significant amount of work on designing and analyzing underwater MAC protocols [4, 5, 12, 13, 14, 6, 7]. While this prior work develops new protocols, here our goal is to understand the fundamental impact of space-time uncertainty in acoustic medium access and propose a framework for analyzing the MAC performance. This understanding, however, suggests adding guard time to slotted ALOHA to improve its throughput underwater.

As for ALOHA protocols in underwater networks, Vieira *et al.* [14] performed simple analysis of slotted ALOHA and reached a conclusion similar to one of ours: slotted ALOHA degrades to pure ALOHA under high latency. Xie *et al.* [6] have compared the performance of ALOHA and CSMA with RTS/CTS mechanism for underwater networks. Gibson *et al.* [7] have extended this work to analyze the performance of ALOHA in a linear multi-hop topology. These papers, however do not attempt to address the following questions: why does pure ALOHA's performance in underwater remain the same as in RF? why does slotted ALOHA's performance degrade to pure ALOHA in the presence of varying propagation delay? How can this degradation be handled and what are the optimal parameters for it? In this paper we specifically address these questions and provide answers.

Theoretical work has begun to explore this direction. Vieira *et al.* [14] analyzed slotted ALOHA and concluded that it degrades to unslotted ALOHA under high propagation delay. Gibson *et al.* [7] have analyzed the performance of ALOHA in a linear multi-hop topology. However, these works do not consider the use of guard times to relieve the negative effect of the large propagation delay.

Adding guard time was previously considered in the design of *sloppy slotted ALOHA* (SSA) [15]. But, SSA was designed for satellite networks with a single, centralized receiver (the satellite). In such networks, they also have considered variable propagation delay, but it's assumed to be induced by the imperfection (or "sloppiness") of each node's implementation, not by the location ofeach node. In fact, nodes are located on the ground, and so, approximately equidistant to the satellite resulting in similar propagation delay for each link. Our work, on the other hand, focuses on ad-hoc acoustic sensor networks where the relative distance to the receiver can vary greatly from node to node.

3. Space-time Uncertainty and the ALOHA Protocol

In this section we summarize the concept of space-time uncertainty with regards to medium access, first introduced in a prior work [12]. We then explore this concept in terms of the ALOHA protocol in a high-latency environment. This exploration provides us with design guidelines for modifying ALOHA for an underwater MAC protocol which we then present in the next section.

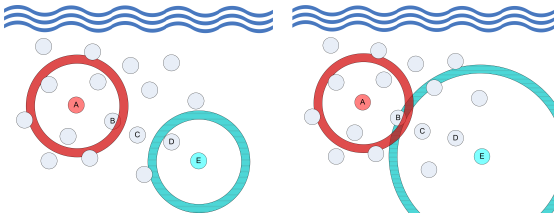

(a) Same transmission time; no collision at B

(b) Different transmission time but collision at B

Figure 1: Illustration of space-time uncertainty

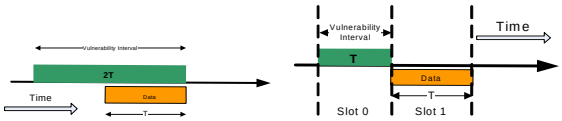

(a) Aloha

(b) Slotted ALOHA

Figure 2: Vulnerability intervals for ALOHA and slotted ALOHA.

3.1. Space-Time Uncertainty

Channel state in short-range RF networks can be estimated quickly since propagation delay is negligible. The large propagation delay of acoustic media makes it essential to also consider the locations of a receiver and potential interferers. Distance between nodes translates into uncertainty of current global channel status: *space-time uncertainty*. Although prior underwater work implicitly considers this uncertainty [5], we present a systematic description of this principle and its impact on contention based medium access. We next give an example of this principle, but separately investigate its impact on ALOHA protocols in detail [10].

Consider Figure 1: the two concurrent transmissions from A and E are received separately at nodes B and D but will collide at node C. This shows that collision and reception in slow networks depend on both transmission *time* and receiver *location*. This space-time uncertainty can also be viewed as a duality where similar collision scenarios can be constructed by varying either the transmission times or the locations of nodes. Although, in principle, this uncertainty occurs in all communication, it is only significant where latency is very high.

We now explore the performance of pure and slotted ALOHA in an underwater, high-latency networked scenario, in the light of our space-time uncertainty principle.

3.2. Analysis of ALOHA with Time Uncertainty

We first refresh the classical analysis of pure and slotted ALOHA protocol [16], where nodes immediately transmit application packets. This analysis was done by assuming collisions with respect to the transmission time alone, thus only considering temporal uncertainty. As collisions matter only at an intended receiver, this analysis has an implied assumption of no propagation delay. If propagation delay is significant this analysis then requires assuming transmitter equidistant to a receiver (as in [9]).

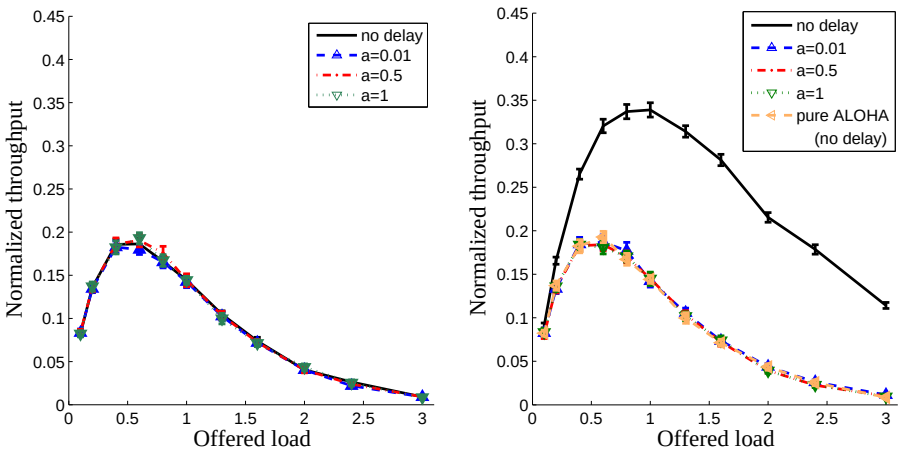

(a) Pure ALOHA (b) Slotted ALOHA

Figure 3: Throughput of pure and slotted ALOHA protocols vs. offered load (packets/transmission time); a is a parameter representing varying maximum propagations by normalizing the delay to the transmission time (more details in Section 5.1). This figure shows that for any value $a > 0$, slotted ALOHA degrades to pure ALOHA in underwater networks.

It further assumes an infinite numbers of nodes, with all arriving packets served at a new node and transmitted immediately into the network. The packets that collide are buffered, making nodes backlogged. Such backlogged nodes retransmit after an exponential delay. The total offered load to the network is thus combination of the Poisson arrival and backlogged exponential retransmissions. This results in a combined Poisson packet arrival process (with mean λ) to the network having normalized throughput $G(n)$ (expected packet/unit time) where n represents the number of backlogged nodes in the network.

The *vulnerability interval (VI)* is defined as the *time* interval relative to a sender's transmission within which another node's transmission causes collision [9]. Assuming T as the packet transmission time, Figure 2(a) shows that the VI is equal to *2T*. On the other hand, slotted ALOHA allows transmission only at the start of synchronized slots of length T. As Figure 2(b) shows, this synchronization ensures that only interfering packets that arrive in slot 0 will result in a collision. It thus reduces the VI from *2T* to T by preventing any cross-slot overlap.

Classical analysis using the concept of vulnerability interval shows that slotted ALOHA achieves maximum normalized throughput of $1/e$ with λ of 1 packet per slot, while pure ALOHA achieves its maximum of $1/2e$ at 0.5 packets/slot [16, 9].

As mentioned above, the classical analysis is carried out with respect to the transmitter's time. The assumption of a single receiver equidistant to all transmitters results in a similar vulnerability interval at the receiver—regardless of the propagation delay (as shown by Klienrock and Tobagi [9]). Strictly speaking, these assumptions do not hold for all ad hoc wireless networks, but with short-range RF networks the variation in delay is small enough that it has virtually no effect on performance (for example,

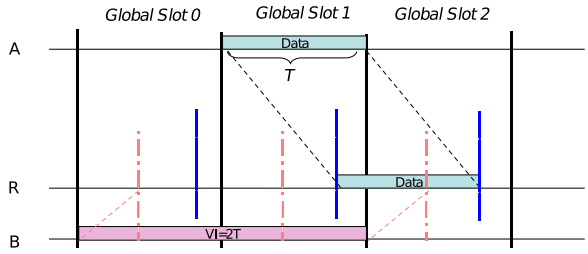

Figure 4: Slotted transmission results in cross slots overlap at receiver.

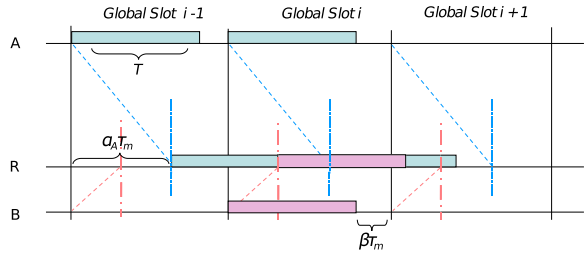

Figure 5: Time diagram of packet transmission using PDT-ALOHA; A and B are transmitters and R is the receiver. B locates closer to the receiver than A.

10μs delay over 25m). In satellite networks delay is long, but there is typically only one sender or receiver. We next show, through simulation and analysis, that the performance of ALOHA can be significantly affected in acoustic networks where these assumptions do not hold.

3.3. ALOHA with Space Uncertainty

In order to understand the impact of location-dependent propagation latency, we now simulate both simple ALOHA and slotted ALOHA with a event-based simulator developed for underwater MAC research [12]. The simulation setting is presented in Section 7.1. Our simulation results (Figure 3 and more details in [10]) showed two interesting results.

First, throughput of pure ALOHA does not change, under any delay regime (Figure 3(a)). This result is explained by looking at packet arrivals at the *receiver*, with and without propagation delay. With no propagation delay the packet arrival at receiver is exactly the same as at transmitter. With propagation delay the arrival time at the receiver is offset by a constant delay. Because the delay is constant for all packets sent by the transmitter, their arrivals at the receiver is still a Poisson process with the same parameter as with no latency. Therefore, with the fact that the sum of independent Poisson processes is indeed a Poisson process, the throughput remains the same in either case. We should point out that pure ALOHA does not attempt to reduce time uncertainty, hence further ignoring space uncertainty has no impact.

The second interesting result is the degradation of slotted ALOHA throughput to that of pure ALOHA when *any* propagation latency is considered, shown by Figure 3(b)

(a similar observation was made by Vieira *et al.* [14]). This is explained by looking at the overlap of globally synchronized slots at a receiver R (Figure 4). Node A's transmission in slot 1 can collide with any packet transmitted by node B in slot 1 (queued at B in previous slot 0) *and* any one transmitted in slot 2 (queued during slot 1).

Generalizing the above example, every transmitter has the collision with the packets sent in the previous consecutive time slot from the transmitters located farther from the receiver, in addition to the collision with the packets sent in the same time slot. Also, every transmitter has another collision with the packets sent in the next consecutive time slot from the transmitters located nearer to the receiver. Hence, when transmitters are deployed uniformly at random in the area, a packet sent from an arbitrary transmitter n_i collides with a packet transmitted in the previous time slot with probability $p_1 = (\text{area farther than } n_i \text{ from } R)/(\text{total area})$. With probability $p_2 = (\text{area nearer than } n_i \text{ from } R)/(\text{total area})$, a packet sent from the transmitter collides with a packet transmitted in the next time slot. The probability that there is another transmitter with the same distance from R is zero because its associated area is zero. And, we have a collision with probability 1 when more than one packet is sent in the same time slot. Therefore, the expected vulnerability interval is $E[VI] = Tp_1 + Tp_2 + T = 2T$ since $p_1 + p_2 = 1$. We use the expected VI because every packet does not collide with every packet sent in the adjoining time slots.

This vulnerability interval is the same as in pure ALOHA, and thus any propagation latency nullifies the benefit of time synchronization. If the network always has a single receiver, and nodes knew their relative locations, it is conceivable for slotting to be made relative to the receiver. However this simplification does not match the ad hoc network paradigm where any node can be a potential receiver.

Radio networks, although having very small propagation latency, *do* undergo a similar performance degradation, as we model any packet overlap as collision. However, most RF systems can usually tolerate an overlap of up to a single bit (depending on coding techniques). As a result for high speed RF networks, if bit rate is 10Mb/s (e.g., IEEE 802.11b), the maximum propagation delay that slotted ALOHA can tolerate is 1ns, or 30m in distance. Thus such systems do not exhibit the immediate performance degradation that we have shown for any propagation delay. On the other hand, acoustic systems even with low data rate modems (1Kb/s [17]) can tolerate only 1ms or 1.5m in distance due to much slower speed of propagation (about 1500m/s). Thus, the impact of spatial uncertainty for slotted ALOHA will be more evident for any acoustic network than it is for RF networks.

4. PDT-ALOHA: the Protocol

We now postulate that space-time uncertainty can be handled by the addition of extra guard time beyond the transmission time in time slots. These guard times are added to ensure a single slot overlap at the receiver, thus *tolerating* the *large propagation delays*. We refer to this modified version as propagation-delay-tolerant ALOHA (PDT-ALOHA). As we argue in Section 3.3 while a centralized network can handle large delays by synchronizing slots at the receiver, a similar solution is not feasible for ad-hoc networks where every node can be a potential receiver.

We first describe the modified protocol and the intuition on how guard time adds tolerance to space-uncertainty. We then describe our methodology to evaluate the protocol with both rigorous mathematical analysis and protocol simulations.

In our modification to slotted ALOHA, nodes still transmit only at the start of globally synchronized slots. Global time synchronization can be achieved using underwater time sync protocols such as [18, 19]. The slot duration, however, is increased from T to $T + \beta \cdot \tau_{max}$, where β represents the fraction of maximum propagation delay (τ_{max}) that nodes wait after finishing their transmission (Figure 5). Hence, $\beta\tau_{max}$ is the guard time, and β can be considered as the *normalized guard time*. Choosing $\beta = 1$ ensures that no overlap at the receiver occurs unless packets are transmitted in the same slot, the guarantee that slotted ALOHA was originally designed to achieve when delay is not important. However this value of β results in a long wait time after each packet that will increase packet transmission latency and bandwidth overhead. With $\beta < 1$ there remains the possibility that some node pairs still have the vulnerability interval of two slot durations (as in Figure 4). Therefore, reducing β value lowers the bandwidth overhead, but increases collision probability. Based on the intuition that the distance between node pairs is often smaller than the maximum propagation delay, we vary β to evaluate the tradeoff between bandwidth overhead and collision probability.

5. Mathematical Analysis of PDT-ALOHA

In this section we analyze the performance of PDT-ALOHA. In particular, we investigate key metrics including probability of collisions, success rate, and throughput.

5.1. Assumptions

We make the following assumptions to analyze the performance of the PDT-ALOHA protocol below, unless stated otherwise.

We consider the one-hop ad-hoc underwater network where the network has one receiver and multiple transmitters. Because the network is ad-hoc, the distance between the receiver and transmitters are not necessarily equidistant. Hence, we assume that the network has one receiver and n transmitters, which are deployed in the two-dimensional disk area. The receiver is located at the center of the disk area, and the transmitters are deployed uniformly at random in the area. We assume the 2D area because we consider the network deployed in the ocean floor.

The propagation speed of communication is a positive finite constant regardless of the location in the network, so that the maximum propagation time τ_m is the propagation time from the receiver to the farthest transmitter. The transmission rate is constant for every transmitter. The packet size is constant so that the transmission time for a packet is constant, which we assume is one (without loss of generality). Only a proper scaling is needed for some parameters, particularly τ_m, in order to cope with the general transmission time. Hence, the normalized maximum propagation delay a to the transmission time is $a = \tau_m/(\text{transmission time}) = \tau_m$.

We assume that the packet arrival per node at a given time slot follows the I.I.D. Bernoulli distribution. Specifically, a transmitter sends a packet to the receiver with probability p in each time slot. Note that this provides discrete approximation to the

Poisson process of the packet arrivals to the network. If the receiver receives more than one packet simultaneously at any time in a time slot, all the packets involved fail to get delivered successfully causing a collision. The links over which transmissions take place are lossless. A transmitter always transmits a packet at the start of the time slot if the transmitter wants to send the packet. All the nodes have globally synchronized time slots. The transmission time is no less than the maximum propagation time so that $a \leq 1$.

The assumption that $a \leq 1$ is to make sure that the collision between a time slot and another is confined to the consecutive time slots. So, with this assumption, there is no possibility that a packet sent in i-th time slot collides with another in j-th time slot, where $j \notin \{i-1, i, i+1\}$.

5.2. Success Rate

In order to analyze the throughput we first derive the expected number of successful packet receptions in a time slot, which we refer to as *success rate*. We use the linearity of expectations and conditional probabilities to calculate the success rate. Let the indicator variable I_i be 1 when the receiver receives the packet from i-th transmitter successfully in the time slot, and 0, otherwise.

Let N denote the random variable of the number of the successful receptions in a time slot. Then, $N = \sum_i I_i$. Hence, the success rate is, by the linearity of expectations and conditional probability, as follows;

$$\begin{aligned} E[N] &= \sum_{i=1}^{n} E[I_i] = \sum_{i=1}^{n} \Pr\{I_i = 1\} \\ &= \sum_{i=1}^{n} \Pr\{\textit{no collision} \mid \textit{i-th sender sends}\} \cdot \Pr\{\textit{i-th sender sends}\} \\ &= n \cdot p \cdot \Pr\{NC|n_i\} \end{aligned} \tag{1}$$

where NC denotes the event 'No Collision' and $NC|n_i$ denotes the event that no collision occurs given that i-th sender transmits. The last equality of the above equations holds since the collision probability is symmetrical among all the senders because each transmiter is assumed to have independent and identical distributions for its spatial location and transmissions, and the probability considers all possible realizations of locations of transmitters.

Therefore, in order to calculate the success rate, we need to find out the probability of no collision for the transmitted packet from the i-th sender whose location is uniform at random over the network area.

5.3. Probability of no collision

As we point out in Section 3, the collision depends not only on the temporal uncertainly, but also on the spacial uncertainty. If more than one node transmit packets in the same time slot, the packets collide with each other regardless of the locations of their transmitters (when $a < 1$). But, collisions can occur even if two packets are transmitted in different time slots, depending on their senders' locations. We call the former collision *intra-timeslot collision*, and the latter *inter-timeslot collision*.

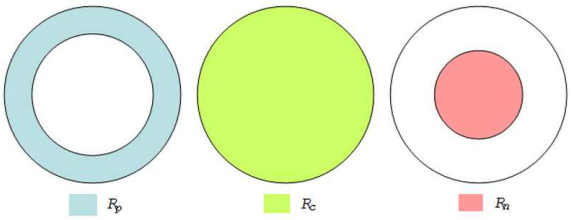

Figure 6: Collision regions: R_p is the region from which packets sent in the previous consecutive time slot would collide with the interested packet, R_c is the region for transmitters for the intra-timeslot collision, and R_n is the region for transmitters in the next time slot for the inter-timeslot collision.

Definition 1. *The **normalized (propagation) time distance** α of sender X from the receiver is the propagation time from the receiver to X divided by the maximum propagation time in the network.*

It turns out that the system can have at most three collision regions for each and every transmitter; one for the intra-timeslot collision and two for the inter-timeslot. In order to identify the regions, let us suppose an arbitrary transmitter n_i which has the normalized time distance of α (Definition 1). Then, the first collision region is the region such that a packet sent from n_i would collide with a packet if it is sent in the previous consecutive time slot by a node in the region. Similarly, the packet from n_i would collide with a packet sent in the same time slot by another node in the second region, and the third region is for the collision with a packet in the next consecutive time slot. We denote the three collision region by $R_p(\alpha), R_c(\alpha), R_n(\alpha)$, respectively, noting that each region depends on the distance of the interested transmitter from the receiver. Moreover, they also depend on the normalized guard time β, but let us omit it in the notation because the omission does not incur ambiguity.

Note that, after calculation, the regions can be expressed in terms of normalized time distance and guard time. The region $R_p(\alpha)$ is where the normalized time distance from the receiver is at least $\alpha + \beta$, but no more than 1. That is, $R_p(\alpha) = \{\mathbf{p}|\alpha + \beta \leq \mathfrak{d}(\mathbf{p}) \leq 1\}$, where $\mathfrak{d}(\mathbf{p})$ denotes the normalized time distance of the point $\mathbf{p}$ from the receiver. Similarly, we have $R_c(\alpha) = \{\mathbf{p}|0 \leq \mathfrak{d}(\mathbf{p}) \leq 1\}$, and $R_n(\alpha) = \{\mathbf{p}|0 \leq \mathfrak{d}(\mathbf{p}) \leq \alpha - \beta\}$. Figure 6 visually presents the regions.

The probability of no collision given a packet sent by an arbitrary i-th sender n_i is then as follows conditioning on the n_i's normalized time distance α;

$$\begin{aligned} \Pr\{NC|n_i\} &= \int_0^1 \Pr\{NC|n_i \text{ transmits}, \mathfrak{d}(\mathbf{p}_i) = \alpha\} \cdot f_{\mathfrak{d}(\mathbf{p}_i)|n_i}(\alpha) d\alpha \\ &= \int_0^1 2\alpha \Pr\{NC|\alpha\} d\alpha, \end{aligned} \tag{2}$$

where $\mathbf{p}_i$ is the location of n_i, $f_{\mathfrak{d}(\mathbf{p}_i)|n_i}(\cdot)$ is the probability density function of the normalized time distance of n_i from the receiver given that n_i transmits, and $NC|\alpha$ is the abbreviated representation of the event that no collision occurs given n_i transmits and its normalized distance from the receiver is α.

The last equation holds because the location of a node is independent of the packet transmission and the transmitters are deployed uniformly in our assumption.

Meanwhile, the probability of no collision of a specific packet does depend on the location of its sender because it defines the three collision regions, $R_n(\alpha)$, $R_c(\alpha)$, and $R_p(\alpha)$; and the regions' areas affect the probability. Hence, further conditioning on the numbers of other transmitters in those three collision regions, we can get the following equation:

$$\begin{aligned}\Pr\{NC|\alpha\} &= \sum_{(x,z):x+z\leq n-1} \begin{matrix}\Pr\{NC \mid \alpha, N_n = x, N_p = z, N_c = n-1\} \\ \times P\{N_n = x, N_p = z, N_c = n-1|\alpha\}\end{matrix} \end{aligned} \quad (3)$$

where N_n, N_c, and N_p denote the number of other transmitters in the collision regions $R_n(\alpha), R_c(\alpha)$, and $R_p(\alpha)$ respectively. Note that (i) $N_c = n-1$ because the intra-timeslot collision region $R_c(\alpha)$ is the whole area in our assumption; and (ii) there are $(n-1)$ other transmitters in total because we focus on one specific transmitter's success.

Note also that the event of $N_n = x, N_p = z, N_c = n-1|\alpha$ has the multinomial distribution with parameters $n-1$, $p_n(\alpha)$, and $p_p(\alpha)$, where $p_i(\alpha),\ i \in \{n, p\}$ denotes the probability that a transmitter lies in $R_i(\alpha)$. And each of these probabilities is the ratio of its area to the entire area of the network; $p_n(\alpha) = (\alpha-\beta)^2$, when $0 < \alpha-\beta < 1$, and $p_p(\alpha) = 1-(\alpha+\beta)^2$, when $0 < \alpha+\beta < 1$. The probabilities are all zero otherwise.

Now we have two cases, each of which has three sub-cases. In the first case A ($0 \leq \beta \leq 0.5$), we have three sub-cases; (i) $0 \leq \alpha \leq \beta$, where $R_n(\alpha) = \emptyset$ so that $p_n(\alpha) = 0$; (ii) $\beta \leq \alpha \leq 1-\beta$, where all three collision regions can have areas larger than zero; and (iii) $1-\beta \leq \alpha \leq 1$, where $R_p(\alpha) = \emptyset$ so that $p_p(\alpha) = 0$. In the other case B ($0.5 \leq \beta \leq 1$), we have another three sub-cases; (i) $0 \leq \alpha \leq 1-\beta$, where $R_n(\alpha) = \emptyset$; (ii) $1-\beta \leq \alpha \leq \beta$, where $R_p(\alpha) = R_n(\alpha) = \emptyset$; and (iii) $\beta \leq \alpha \leq 1$, where $R_p(\alpha) = \emptyset$.

Let us consider Case A.(i) first. In this case, the conditional probability of no collision turns out to involve the binomial series as follows;

$$\begin{aligned}\Pr\{NC|\alpha\} &= \sum_{z=0}^{n-1} \Pr\{NC|\alpha, N_p = z, N_c = n-1, N_n = 0\} \cdot \Pr\{N_p = z|\alpha\} \\ &= \sum_{z=0}^{n-1} \binom{n-1}{z} (1-p)^z (1-p)^{n-1} \cdot (1-(\alpha+\beta)^2)^z ((\alpha+\beta)^2)^{n-1-z} \\ &= (1-p)^{n-1}(1-p+p(\alpha+\beta)^2)^{n-1} \end{aligned} \quad (4)$$

Equation (5) and (6) are the summary after calculating the other cases in a similar way.

In Case A,

$$\Pr\{NC|\alpha\} = \begin{cases} (1-p)^{n-1}(1-p+p(\alpha+\beta)^2)^{n-1}, & \textit{if } 0 \leq \alpha \leq \beta \\ (1-p)^{n-1}(1-p+4p\alpha\beta)^{n-1}, & \textit{if } \beta \leq \alpha \leq 1-\beta \\ (1-p)^{n-1}(1-p(\alpha-\beta)^2)^{n-1}, & \textit{if } 1-\beta \leq \alpha \leq 1 \end{cases} \quad (5)$$

In Case B,

$$\Pr\{NC|\alpha\} = \begin{cases} (1-p)^{n-1}(1-p+p(\alpha+\beta)^2)^{n-1}, & \text{if } 0 \le \alpha \le 1-\beta \\ (1-p)^{n-1}, & \text{if } 1-\beta \le \alpha \le \beta \\ (1-p)^{n-1}(1-p(\alpha-\beta)^2)^{n-1}, & \text{if } \beta \le \alpha \le 1 \end{cases} \quad (6)$$

Substituting (5) or (6) into (2) we can obtain the expression for the probability of no collision which can be evaluated easily with the numerical method.

Note that the expression for probability of no collision does not involve the maximum propagation delay τ_m implying the probability is independent of τ_m so that the success rate is also independent of τ_m. It turns out from Theorem 1 that the success rate is independent of τ_m even after relaxing the assumption of 2D unit disk of the network and the identical distribution of packet transmission for each node.

Theorem 1. *Suppose a network of nodes with fixed spatial locations of nodes, a fixed transmission probability p_i in a time slot for each node i, and a transmission time T for a packet. Then, the success rate f is independent of the maximum propagation time τ_m in the network as long as $0 < \tau_m \le T$. In other words, it is independent of the propagation speed v_p.*

PROOF. Since the spatial locations of nodes are fixed, the spatial distance r_m from the receiver to the farthest node is constant; $r_m = \tau_m \cdot v_p = \textit{const.}$

The spatial distance r_i of an arbitrary i-th transmitter is also fixed, and so the normalized propagation time delay α_i of the node is constant regardless of r_m as long as $r_m > 0$ or $0 < v_p < \infty$ because of the following:

$$r_i = \alpha_i \cdot \tau_m \cdot v_p = \alpha_i \cdot r_m \quad \Rightarrow \quad \alpha_i = \frac{r_i}{r_m} = \textit{const.}$$

Let $r(R_i)$ denote the spatial region associate with the collision region R_i. Then, the spatial region of R_n, R_c, and R_p are all fixed regardless of τ_m because

$$\begin{aligned} r(R_n) &= \{r : 0 \le r \le (\alpha_i - \beta)\tau_m v_p = (\alpha_i - \beta) r_m\} \\ r(R_c) &= \{r : 0 \le r \le \tau_m v_p = r_m\} \\ r(R_p) &= \{r : (\alpha_i + \beta) r_m \le r \le r_m\} \end{aligned}$$

and α_i, β, and r_m are all constants.

Hence, the number of nodes in each of R_n, R_c, and R_p is constant regardless of the speed of propagation, and so the probability of no collision of the i-th transmitter is constant. Therefore,

$$f = \sum_i p_i \Pr\{NC|n_i\} = \textit{const. with respect to } \tau_m$$ □

5.4. Throughput for finite number of nodes

In this paper we consider the throughput S in packets per transmission time. Because the size of time slot is $1 + \beta a$, S can be expressed as follows:

$$S(n, \beta, p, a) = \frac{f(n, \beta, p)}{1 + \beta a} = \frac{np \Pr\{NC|n_i\}}{1 + \beta a} \quad (7)$$

$$\begin{aligned}
\lim_{n\to\infty}\left(1-\frac{\lambda}{n}\right)^{n-1} &= e^{-\lambda} \\
\lim_{n\to\infty}\left(1-\frac{\lambda}{n}+\frac{\lambda}{n}(\alpha+\beta)^2\right)^{n-1} &= e^{-\lambda+\lambda(\alpha+\beta)^2} \\
\lim_{n\to\infty}\left(1-\frac{\lambda}{n}+4\frac{\lambda}{n}\alpha\beta\right)^{n-1} &= e^{-\lambda+4\lambda\alpha\beta} \\
\lim_{n\to\infty}\left(1-\frac{\lambda}{n}(\alpha-\beta)^2\right)^{n-1} &= e^{-\lambda(\alpha-\beta)^2}
\end{aligned}$$

Table 1: Equalities to use as building blocks to calculate the throughput in the limiting case

a	0.2464	p_1	0.1805	p	0.0784	p_2	0.2257
b	-2.9312	q_1	0.6543	q	0.2638	q_2	0.6959
c	-0.9887	r_1	0.8898	r	0.9173	r_2	0.9049

Table 2: Constants for Approximation Models

, where $f(n,\beta,p)$ is the success rate and we know the probability of no collision from the previous section.

5.5. Throughput for infinite number of nodes

In this section, we investigate the throughput of PDT-ALOHA protocol with an infinite number of nodes with the traffic load λ over the network, i.e, $n\to\infty$ while $p=\lambda/n$. Hence, the throughput in this case is given by

$$S(\beta,\lambda,a)=\lim_{n\to\infty}S|_{p=\frac{\lambda}{n}}=\frac{\lambda}{1+\beta a}\lim_{n\to\infty}\Pr\{NC|n_i\} \tag{8}$$

Because the integrand of (2) converges uniformly over $[0,1]$ (see Appendix), we can exchange integral and limit operations by Theorem 7.16 of [20]. Hence, with the equalities in Table 1, we can achieve the conditional probability of no collision in this limiting case as follows:

If $0\le\beta\le 0.5$;

$$\Pr\{NC|\alpha\}=\begin{cases}e^{-2\lambda+\lambda(\alpha+\beta)^2}, & 0\le\alpha\le\beta\\ e^{-2\lambda+4\lambda\alpha\beta}, & \beta\le\alpha\le 1-\beta\\ e^{-\lambda-\lambda(\alpha-\beta)^2}, & 1-\beta\le\alpha\le 1\end{cases} \tag{9}$$

If $0.5<\beta\le 1$;

$$\Pr\{NC|\alpha\}=\begin{cases}e^{-2\lambda+\lambda(\alpha+\beta)^2}, & 0\le\alpha\le 1-\beta\\ e^{-\lambda}, & 1-\beta\le\alpha\le\beta\\ e^{-\lambda-\lambda(\alpha-\beta)^2}, & \beta\le\alpha\le 1\end{cases} \tag{10}$$

Therefore, substituting (9) or (10) into (2) which can be numerically evaluated easily, we can obtain the expression for the probability of no collision for a packet of

a transmitter. We shall use numerical evaluations to investigate the properties of the maximum throughput and obtain a very simple approximation for it in Section 6.2.

5.6. Throughput with no guard time

We derive the throughput of PDT-ALOHA for the case where there is no guard time (i.e. $\beta = 0$) and the number of nodes is infinite, using our derivation for the general case developed in previous sections. We present this as a sanity check because we know that, without the guard time, the PDT-ALOHA is equivalent to the traditional slotted ALOHA, whose performace degrades to that of the pure (unslotted) ALOHA given by (as discussed in Section 3.3)

$$Th_{pure} = \lambda e^{-2\lambda} \tag{11}$$

For our derivation, no guard time ($\beta = 0$) implies $\Pr\{NC|\alpha\} = e^{-2\lambda}$ from (9), which in turn impies from (2)

$$\Pr\{NC|n_i\} = \int_0^1 2\alpha e^{-2\lambda} d\alpha = e^{-2\lambda} \tag{12}$$

Therefore, the throughput of PDT-ALOHA is given from (8) by

$$S(\beta = 0, \lambda, a) = \lambda e^{-2\lambda} \tag{13}$$

This shows our derivation correctly capture the throughput mechanism for the no-gaurd-time case and the phenomenon that the amount of maximum propagation time becomes irrelevant to the throughput when there is no guard time for PDT-ALOHA.

6. Optimization of PDT-ALOHA

In this section we investigate the *maximum* success rate and the *maximum* throughput of PDT-ALOHA protocol. We also have an interest in the protocol parameters, particularly the size of guard time and the traffic load, which realize the maximum throughput.

We consider the traffic load per transmission time λ_r as well as the load per time slot λ because it is useful to compare traffic loads between systems of different size of time slot. And, it turns out it gives simpler approximation for the optimum values. These two kinds of traffic load have the relationship as $\lambda_r = \lambda/(1 + \beta a)$.

Although we assume in this section the limiting case, where the number of nodes in the network is infinite, it is fairly straightforward to adapt the method we used here for the finite number of nodes.

6.1. Special Cases

We start with special cases, i.e. $\beta = 0$, or $\beta = 1$, which can be analyzed analytically. Then, we examine general cases given a network size in terms of the maximum propagation delay in Section 6.2.

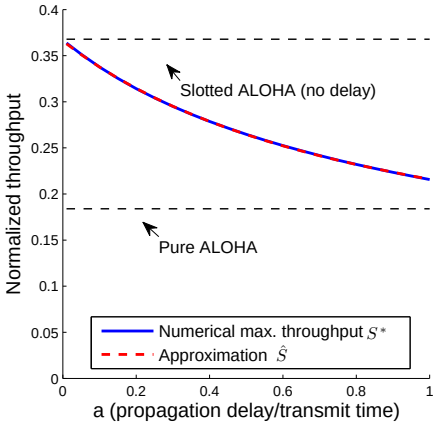

Figure 7: Maximum throughputs of PDT-ALOHA depending on the guard time size

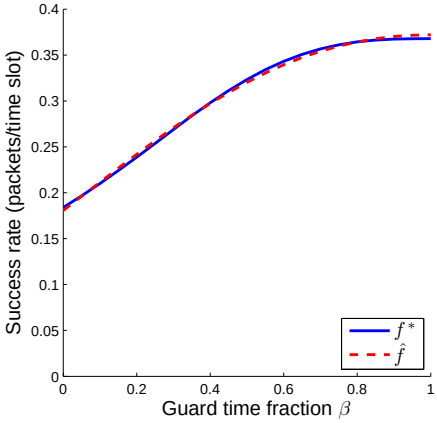

Figure 8: The maximum success rate; numerically calculated values of f^* and its approximation $\hat{f}$

In these special cases, the maximum throughput is associated with a given fixed β, and defined as: $S^*(\beta, a) = \max_{\lambda \in \mathbb{R}^+} S(\beta, \lambda, a)$

When there is no guard time ($\beta = 0$) or the guard time is full so that there is no collision between packets from different time slots ($\beta = 1$) we have a closed-form expression for throughput which is simple enough to analyze analytically the maximum throughput. When $\beta = 0$, the throughput is $S_0(\lambda) \doteq S(\beta = 0, \lambda, a) = \lambda e^{-2\lambda}$ from (13).

The maximum throughput can be obtained simply using the derivative since S_0 is convex. The maximum is achieved at $\lambda = 0.5$ (i.e. $\lambda_r = 0.5$) as follows:

$$S_0^* = S^*(\beta = 0, a) = e^{-1}/2 \tag{14}$$

When $\beta = 1$ the throughput is $S_1(\lambda, a) \doteq S(\beta = 1, \lambda, a) = \frac{\lambda e^{-\lambda}}{1+a}$ from (2), (8), and (10).

Because S_1 is convex regarding λ at any $a \in (0, 1]$, we can obtain its maximum given a using the partial derivative as follows:

$$S_1^*(a) = S^*(\beta = 1, a) = \frac{e^{-1}}{1+a} \tag{15}$$

where the maximizer is $\lambda = 1$ while the corresponding traffic load per transmission time is $\lambda_r = 1/(1+a)$.

6.2. Maximum Throughput

The maximum throughput in this general case is not conditioned on the guard time. Hence, it is defined as: $S^*(a) = \max_{(\beta,\lambda) \in \mathbb{R}^+ \times \mathbb{R}^+} S(\beta, \lambda, a)$.

Because it is very hard to obtain the closed form expression for the general case (if possible), we resort to use the numerical method to analyze the optimum behav-

ior of the system. Based on the result of the numerical analysis, we propose simple approximations for the optimum behavior and its protocol parameters.

Now we investigate the maximum throughput $S^*(a)$ over all possible non-negative guard time β and network load per time slot λ given the network size in terms of the maximum propagation delay. Note that it is sufficient to look into only $\beta \in [0,1]$ and $\lambda \in [0,1]$ because $S(\beta,\lambda,a) \le S(1,1,a)$, $\forall\beta \ge 1$, $\forall\lambda \ge 1$ due to Theorem 2 (for a finite number of nodes), Theorem 3 (for an infinite number of nodes), and Theorem 4.

Theorem 2. *Suppose a network of n number of nodes is assumed as that of Section 5.4 with $p = \lambda/n$. Then, the throughput S_n of the PDT-ALOHA protocol with $\lambda \ge 1$ for the network is no higher than when $\lambda = 1$. That is,*

$$\lambda \ge 1 \;\Rightarrow\; S_n(\beta,\lambda,\tau_m) \le S_n(\beta,1,\tau_m),\ \forall\beta \in [0,1]$$

PROOF. The success rate $f_n(\beta,\lambda)$ can be expressed as follows using (1), (2), (5), and (6):

$$f_n(\beta,\lambda) = \lambda \int_0^1 2\alpha \Pr\{NC|\alpha\} d\alpha = \lambda \left(1-\frac{\lambda}{n}\right)^{n-1} \int_0^1 g_n(\beta,\lambda) d\alpha$$

where $g_n(\beta,\lambda)$ is a proper function after extracting $\left(1-\frac{\lambda}{n}\right)^{n-1}$.

Suppose $\lambda \ge 1$. Since $0 < \lambda_1 \le \lambda_2 < n$ implies $g_n(\beta,\lambda_1) \ge g_n(\beta,\lambda_2)$ for all $\beta \in [0,1]$,

$$\begin{aligned} f_n(\beta,\lambda) &= \lambda \left(1-\frac{\lambda}{n}\right)^{n-1} \int_0^1 g_n(\beta,\lambda) d\alpha \\ &\le \lambda \left(1-\frac{\lambda}{n}\right)^{n-1} \int_0^1 g_n(\beta,1) d\alpha \;\le\; \left(1-\frac{1}{n}\right)^{n-1} \int_0^1 g_n(\beta,1) d\alpha \;=\; f_n(\beta,1) \end{aligned}$$

where the last inequality holds since $x(1-x/n)^{n-1} \le (1-1/n)^{n-1}$ for $\forall x \ge 1$ and $\forall n \ge 2$.

Therefore,

$$S_n(\beta,\lambda,\tau_m) = \frac{f_n(\beta,\lambda)}{1+\beta\tau_m} \le \frac{f_n(\beta,1)}{1+\beta\tau_m} = S_n(\beta,1,\tau_m) \qquad \square$$

Theorem 3. *Theorem 2 holds for the infinite number of nodes as long as the throughput limit exists.*

PROOF. Since $S_n(\beta,\lambda,\tau_m) \le S_n(\beta,1,\tau_m)$ for $\forall\lambda \ge 1$ and $\forall n \ge 2$ from Theorem 2,

$$S(\beta,\lambda,\tau_m) = \lim_{n\to\infty} S_n(\beta,\lambda,\tau_m) \le \lim_{n\to\infty} S_n(\beta,1,\tau_m) = S(\beta,1,\tau_m)$$

as long as the limits exist. $\square$

Theorem 4. *The throughput S with the normalized guard band size $\beta \ge 1$ of an arbitrary network is no higher than that of $\beta = 1$. That is,*

$$\beta \ge 1 \;\Rightarrow\; S(\beta,\vec{p},\tau_m) \le S(1,\vec{p},\tau_m)$$

PROOF. If $\beta \geq 1$, there is no longer collision of packets between different time slots and β does not have any effect on packets sent in the same time slot. Hence, the success rate is same for $\beta \geq 1$ as that of $\beta = 1$. However, increasing β makes the size of time slot increases. Therefore, the claim follows. □

We evaluate the maximum throughput S^* for 21 values of τ_m starting from 0.01 to 1 using the numerical method. After examining the behavior of S^*, we have found out that the following simple expression can approximate S^* quite closely:

$$\hat{S}(a) = p + \frac{q}{a + r} \tag{16}$$

where p, q, and r are constants. The curve-fitted values for the constants are presented in Table 2.

Figure 7 shows the accuracy of the approximation; The plot for S^* is the interpolation of 21 data points of the maximum throughput over offered loads and guard times found by numerical methods. As can be seen, our approximation has reasonably good accuracy. Quantitatively, it does not deviate more than 0.3% from the numerical evaluations of S^*.

The optimum values of protocol parameters which realize the optimum throughput are also of interest. In particular, we are interested in the optimum size of the guard time β^* and the optimum traffic load λ_r^* per transmission time given the network size in terms of a. Through the numerical analysis we have found out that the optimizer β^* and λ_r^* can be closely approximated with the following models:

$$\hat{\beta}(a) = p_1 + \frac{q_1}{a + r_1} \tag{17}$$

$$\hat{\lambda_r}(a) = p_2 + \frac{q_2}{a + r_2} \tag{18}$$

where p_i, q_i, and $r_i, \forall i \in \{1, 2\}$ are constants; their proper values are given in Table 2 through curve fitting.

Figure 9 pictorially presents optimizers β^* and λ_r^*, and their approximations depending on the maximum propagation delay a. It also shows the guard time βa normalized to the transmission time, which is one in our paper. As can be seen, our approximations are very close to their numerical counterparts, respectively; $\hat{\beta}$ deviates no more than 2% while $\hat{\lambda_r}$ differs no more than 0.2%. We can also see that the optimum guard time is less than roughly half of the transmission time, and it is monotonically increasing as the maximum propagation delay increases.

6.3. Maximum success rate

In this subsection we consider the maximum success rate. We first present the analytic findings about the properties of the maximum number of successful receptions. The findings are more general than what we assume previously. We find out through Theorem 6 that, as long as the maximum propagation delay is less than the transmission time of a packet, the maximum success rate is monotonically non-decreasing with respect to the guard time β even when the network area is no longer 2D disk and the sending probability is not identical for each node.

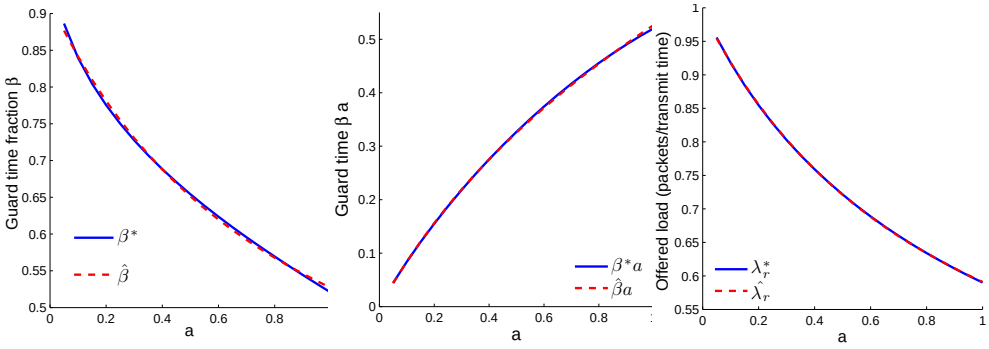

(a) (b) (c)

Figure 9: Numerically calculated optimizers and their approximations vs. the normalized maximum propagation delay a (propagation delay / transmission time), (a) for guard time fraction β, (b) for traffic load λ_r per transmission time

Lemma 5. *Given the arbitrary location distribution of n transmitters and the probability p_i that i-th transmitter transmits a packet in a time slot, the success rate $f(\beta, \vec{p})$ is monotonically non-decreasing as the normalized guard time β increases when the maximum propagation delay τ_m in the network is less than the transmission time T.*

In other words, $0 \leq \beta_1 \leq \beta_2 \leq 1 \Rightarrow f(\beta_1, \vec{p}) \leq f(\beta_2, \vec{p})$*, for all* $\vec{p} = (p_1, \ldots, p_n)$ *s.t.* $0 \leq p_i \leq 1, \forall i \in \{1, \ldots, n\}$.

PROOF. Because $\tau_m \leq T$, a transmission can interfere only with the transmission of immediate previous, current, and/or immediate next time slot. Hence, there are at most three collision regions given a transmitter as we investigated in Section 5.3. The three regions for an arbitrary i-th transmitter which has the normalized propagation time distance of α_i are in summary as follows in terms of normalized time distance; $R_n(\alpha_i) = \{\mathbf{p} | 0 \leq \mathfrak{d}(\mathbf{p}) \leq \alpha_i - \beta\}$, $R_c(\alpha_i) = \{\mathbf{p} | 0 \leq \mathfrak{d}(\mathbf{p}) \leq 1\}$, and $R_p(\alpha_i) = \{\mathbf{p} | \alpha_i + \beta \leq \mathfrak{d}(\mathbf{p}) \leq 1\}$

Hence, when β increases, $R_n(\alpha_i)$ decreases monotonically up to $\emptyset$, making the corresponding collision probability monotonically non-increasing; $R_c(\alpha_i)$ stays constant, not changing the probability; and $R_p(\alpha_i)$ decreases monotonically up to $\emptyset$, making the probability monotonically non-increasing. These implies that the probability of no collision for the i-th transmitter $\Pr\{NC | n_i\}$ is monotonically non-decreasing for each i.

Therefore, the success rate $f(\beta, \vec{p}) = \sum_i p_i \Pr\{NC | n_i\}$ is monotonically non-decreasing with respect to β. □

Theorem 6. *With the same assumptions of Lemma 5, the maximum success rate $f^*(\beta)$ over $\vec{p}$ (i.e. $f^*(\beta) = \max_{\vec{p}} f(\beta, \vec{p})$) is monotonically non-decreasing with respect to the normalized guard time size β.*

In other words, $0 \leq \beta_1 \leq \beta_2 \leq 1 \Rightarrow f^*(\beta_1) \leq f^*(\beta_2)$

PROOF. From the definition of f^* and Lemma 5,

$$f^*(\beta_2) \geq f(\beta_2, \vec{p}) \geq f(\beta_1, \vec{p}),\ \forall \vec{p}$$

Therefore, $f^*(\beta_2)$ is an upper bound of $f(\beta_1, \vec{p})$ for all $\vec{p}$, which implies the following:

$$f^*(\beta_2) \geq \max_{\vec{p}} f(\beta_1, \vec{p}) = f^*(\beta_1)$$ □

As in the previous subsection, we use the numerical method to evaluate f^*. The black solid line of Figure 8 shows the interpolation of 22 data points of f^* found numerically.

Although it is hard to obtain the exact expression of f^*, we know from Theorem 6 that the maximized function $f^*(\beta) = \max_\lambda f(\beta, \lambda)$ is monotonically non-decreasing. From this fact and the observation that the log-scale plot of the numerically evaluated $f^*(\beta)$ is approximately of cubic function, we are able to propose the following approximation model for $f^*(\beta)$:

$$\hat{f}(\beta) = e^{a(\beta-1)^2(\beta+b)+c} \tag{19}$$

where a, b, and c are constants and the constraint that $b < -1$ makes sure that the function is monotonically increasing.

The red dashed line of Figure 8 shows this approximation with proper constants suggested in Table 2, as determined through numerical curve fitting.

7. Analysis and Comparison with Protocol Simulation

We now analyze the results of optimal throughput of PDT-ALOHA obtained in previous section to observe the effect of guard time and network delay regime. Furthermore, for comparison we simulate PDT-ALOHA to verify the correctness of our analysis in a realistic network. We first introduce the parameters of the simulation used for comparison and then focus on the results. We end this section by drawing some interesting conclusions from these results.

7.1. Simulation Parameters and Assumptions

We run our simulations using a custom-built, packet-level simulator designed for UWSN MAC research [12][1]. Our simulation scenario consists of a single receiver that does not transmit, with nodes randomly deployed in a circular region with a radius equal to the maximum propagation delay. Nodes, with a single packet buffer, transmit based on an offered load to the network modeled as a Poisson process, with mean ranging from 0 to 3 packets/transmission time, and we only observe the packets successfully received at our designated receiver. We choose a single receiver to parallel our analysis of protocol behavior, but have verified that our results hold with packets reception at other nodes in the network. Protocol performance is evaluated through

[1]This simulator is available from the authors at `http://www.isi.edu/ilense/software/`.

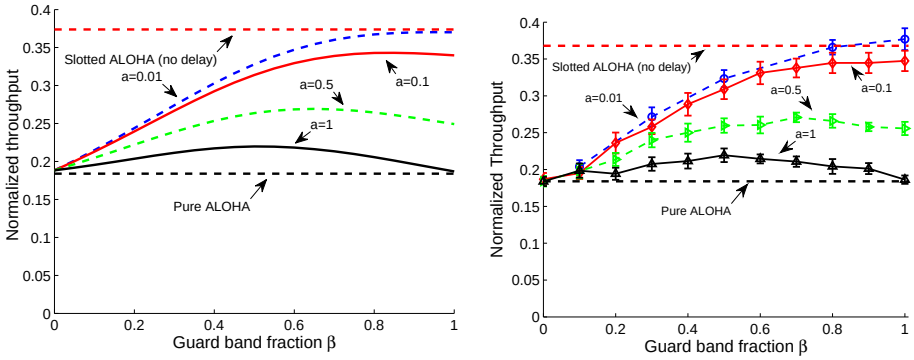

(a) Analytical result (b) Simulation result

Figure 10: Throughput of PDT-ALOHA as guard time length β is varied.

throughput normalized to channel bandwidth. Simulations are run with 32 nodes unless otherwise noted. We use a packet length of 125 bytes, resulting in a transmission time of 1 second (at 1kb/s) to normalize our throughput analysis. We also assume a constant speed of sound as 1500m/s. We alter the maximum range to simulate different delay regimes. Each simulation data point is the averaged result of 25 simulation runs with error bars showing 95% confidence intervals.

7.2. Effect of Guard Time on Throughput

We now look at the maximum achievable throughput (throughput capacity) that PDT-ALOHA can achieve (at an optimal offered load) as a function of guard time length, β which is a fraction of the maximum propagation delay.

Figure 10(a) shows this function of β as the throughput capacity for a fixed n (32 nodes) using numerical methods for maximizing (7) over p. We plot the response for different delay regimes characterized by different values of a. Figure 10(b) shows the plot for the exact same parameters. However, here instead of using analysis we derive our results from empirical data collected from simulations. As we see results from both simulation and analysis compliment each other. Both results show that throughput capacity of a network can be increased by using PDT-ALOHA and that the benefit of the guard time is highly correlated to its size and the delay regime in which the network is operating. We also observe two trends as β increases. First, with very small $a =$ (e.g. 0.01 in simulation results) we see the throughput increases (approaching the optimum) as larger guard time is used due to a decreased inter-timeslot collision probability. Conversely, with large a (e.g. equal to 1 when the propagation delay equals transmission time) the throughput becomes insensitive to the use of guard time. Furthermore, simulation results (not shown here for clarity) show that for any value of a beyond 1, the benefit of choosing additional guard time diminishes. Thus, choosing a packet length that normalizes the propagation delay to an appropriate value is essentially to yield the benefits of PDT-ALOHA.

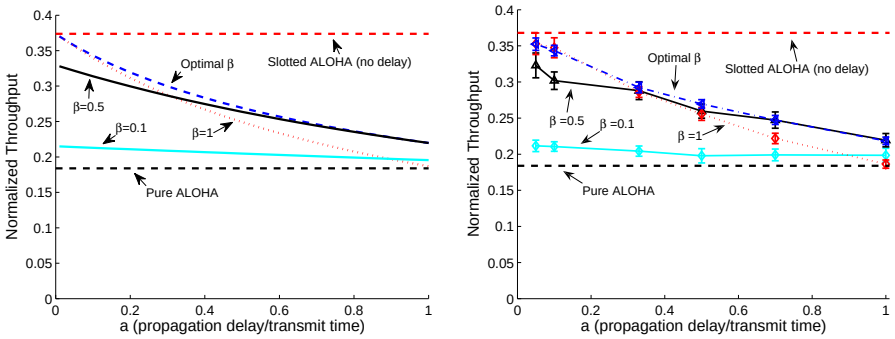

(a) Analytical result (b) Simulation result

Figure 11: Maximum throughput of PDT-ALOHA as the normalized propagation delay a is varied.

7.3. Effect of Delay Regimes on Throughput

We next vary a to observe how the the throughput capacity is affected by propagation delay in PDT-ALOHA. We generate a figure similar to Kleinrock and Tobagi's (Figure 10 in [9]) that shows the impact of propagation delay on throughput capacity for different MAC protocols. However, due to their equidistant and single receiver assumption the authors there showed the capacity of slotted ALOHA not affected by latency, which we have shown to be incorrect for general ad hoc networks in Section 3.3.

Figure 11(a) shows throughput capacity $S^*(\beta, a)$ as a function of the normalized maximum propagation delay a when the guard time β is given and fixed. They are obtained for $n = 32$ maximizing (7) over p with given β and a. For comparison, we have the same plot generated from simulation results in Figure 11(b). We plot the response using different values of β. We also show the β-*optimal* throughput capacity curve $S^*(a)$ using the value of β that maximizes the throughput capacity at a given value of a (using similar methods as in Section 6.2 with (7)). It can be seen that a fixed value of β might lead to a suboptimal throughput. When $\beta = 0.5$, PDT-ALOHA is closest to the β-optimal curve when a is near 1 but the gap increases as a goes to 0. Conversely, for $\beta = 1$ PDT-ALOHA is closest to the β-optimal curve for smaller values of a but becomes inefficient as a approaches 1.

Although the throughput decreases monotonically with increasing values of a, we observe very little sensitivity to a with smaller β values. This insensitivity is due to limited collision prevention provided by shorter guard time. Also the monotonically decreasing slope increases with β causing throughput to become more sensitive to a. Figure 11 shows that PDT-ALOHA can achieve about 17% (when $a = 1$) to 100% (when $a \to 0$) improvement on throughput over vanilla slotted ALOHA in an underwater environment.

Figure 11 shows the normalized throughput in terms of the maximum propagation delay a. Next, let us look into how the maximum throughput changes in terms of the guard time βa. We have found from the numerical analysis that, given a guard time βa in $[0, 1]$, the maximum throughput can be obtained with $\beta = 1$ (hence, $a = \beta a$). This makes the guard time a in this case. Hence, the red dotted line representing the case

$\beta = 1$ in Figure 11 also shows the maximum throughput in terms of the guard time $\beta a = a$.

7.4. Short Hops are Better

Our analytical and simulation results also show higher throughput can be achieved by using guard time for lower values of a. For example, assume we use an acoustic modem that has a communication range of 300m and a speed of 1Kb/s [17]. If we use packet length of 250 bytes, a will be 0.1, and the modified slotted ALOHA can achieve performance similar to the slotted ALOHA in RF networks. Thus in terms of how much of throughput can be reclaimed, shorter communication hops will provide higher throughput benefit.

This conclusion is complimentary to the physical layer argument presented by Stojanovic that higher throughput in acoustic networks can be obtained using smaller hops [21]. Similar arguments from an information theoretic perspective have also been forwarded for bit level [22] and multi-hop [23] underwater acoustic networks. All these results, along with the results in this paper, reinforce the benefit of short-range communication in underwater networks, for reasons beyond energy efficiency.

8. Conclusion

In this paper, we have explored the impact of spatio-temporal uncertainty on UWSN MAC protocols. For such networks, we have shown that location-dependent acoustic propagation delay significantly affects MAC protocols such as slotted ALOHA. Thus it is necessary to consider both space and time uncertainties while designing MAC protocols under varying latency environment of an acoustic UWSN.

We propose PDT-ALOHA to deal with the spatio-temporal uncertainty in slotted ALOHA by adding guard times each slots. We have investigated different metrics of its performance — success rate, throughput, and their optimal values— using both mathematical analysis and protocol simulations. Our results show that the throughput capacity of PDT-ALOHA is 17-100% better than that of simple slotted ALOHA in an underwater environment. We have shown that for the optimal throughput capacity the value of optimal β changes based on operating delay regime. Our results indicate a significant throughput benefit when shorter communication links are used. This argues for deploying dense, short range, multi-hop networks as opposed to sparse and long range networks currently used in underwater networks.

Because underwater networks often face limited energy constraints, it would also be desirable to explicitly consider the energy-efficiency in designing a MAC protocol. However, this work focuses on capturing the impact of latency on ALOHA-like protocols and understanding the mechanics of underwater medium access. Since ALOHA itself was never meant to be energy efficient and PDT-ALOHA does not consider any optimization for energy, the energy-efficiency of PDT-ALOHA remains an open question that should be investigated in future work.

9. Acknowledgement

This research is partially supported by the National Science Foundation (NSF) under grants NeTS-NOSS-0435517, CNS-0708946, and CNS-0821750 and the CAREER award CNS-0347621, by a hardware donation from Intel Co., and by Chevron Co. through the USC Center for Interactive Smart Oilfield Technologies (CiSoft)

References

[1] I. F. Akyildiz, D. Pompili, T. Melodia, Underwater acoustic sensor networks: research challenges, Ad Hoc Networks Journal 3 (3) (2005) 257–279.

[2] J. Heidemann, W. Ye, J. Wills, A. Syed, Y. Li, Research challenges and applications for underwater sensor networking, in: Proceedings of the IEEE Wireless Communications and Networking Conference, 2006.

[3] J. Partan, J. Kurose, B. N. Levine, A survey of practical issues in underwater networks, in: Proceedings of the 1st ACM International Workshop on Underwater Networks (WUWNet'06), ACM Press, New York, NY, USA, 2006, pp. 17–24.

[4] V. Rodoplu, M. K. Park, An energy-efficient MAC protocol for underwater wireless acoustic networks, in: Proceedings of the MTS/IEEE OCEANS'05 Conference, Washington DC, USA, 2005, pp. 1198–1203.

[5] M. Molins, M. Stojanovic, Slotted FAMA: A MAC protocol for underwater acoustic networks, in: Proceedings of the IEEE OCEANS'06 Asia Conference, Singapore, 2006.

[6] P. Xie, J.-H. Cui, Exploring random access and handshaking techniques in large-scale underwater wireless acoustic sensor networks, in: Proceedings of the MTS/IEEE OCEANS Conference, Boston, Massachusetts, 2006, pp. 1–6.

[7] J. H. Gibson, G. G. Xie, Y. Xiao, H. Chen, Analyzing the performance of multi-hop underwater acoustic sensor networks, in: Proceedings of the MTS/IEEE OCEANS Conference, Aberdeen, Scotland, 2007.

[8] N. Abramson, The ALOHA system, in: Proceedings of AFIPS 1970 Fall Joint Computer Conference, Vol. 37, 1970, pp. 281–285.

[9] L. Kleinrock, F. Tobagi, Packet switching in radio channels: Part I - carrier sense multiple access modes and their throughput delay characteristics, IEEE Transactions on Computing 23 (12) (1975) 1400–1416.

[10] A. Syed, W. Ye, B. Krishnamachari, J. Heidemann, Understanding spatio-temporal uncertainty in medium access with aloha protocols, in: Proceedings of the Second ACM International Workshop on UnderWater Networks (WUWNet), ACM, Montreal, Quebec, Canada, 2007.

[11] J. Ahn, B. Krishnamachari, Performance of Propagation Delay Tolerant ALOHA Protocol for Underwater Wireless Networks, in: The 4th IEEE International Conference on Distributed Computing in Sensor Systems (DCOSS '08), 2008.

[12] A. A. Syed, W. Ye, J. Heidemann, T-Lohi: A new class of MAC protocols for underwater acoustic sensor networks, in: Proceedings of the IEEE Infocom, Pheonix, AZ, 2008, pp. 231–235.

[13] B. Peleato, M. Stojanovic, A MAC protocol for ad-hoc underwater acoustic sensor networks, in: Proceedings of the 1st ACM International Workshop on Underwater Networks (WUWNet'06), 2006.

[14] L. F. M. Vieira, J. Kong, U. Lee, M. Gerla, Analysis of ALOHA protocols for underwater acoustic sensor networks, in: Extended abstract from WUWNet'06, 2006.

[15] S. Crozier, P. Webster, Performance of 2-dimensional sloppy-slotted ALOHA random accesssignaling, Wireless Communications, Conference Proceedings, IEEE International Conference on Selected Topics in (1992) 383–386.

[16] D. Bertsekas, R. Gallager, Data Networks, 2nd Edition, Prentice Hall, 1996.

[17] J. Wills, W. Ye, J. Heidemann, Low-power acoustic modem for dense underwater sensor networks, in: Proceedings of the First ACM International Workshop on UnderWater Networks (WUWNet), 2006.

[18] A. Syed, J. Heidemann, Time synchronization for high latency acoustic networks, in: Proceedings of the IEEE Infocom, Barcelona, Catalunya, Spain, 2006.

[19] N. Chirdchoo, W.-S. Soh, K. C. Chua, Mu-sync: a time synchronization protocol for underwater mobile networks, in: WuWNeT '08: Proceedings of the third ACM international workshop on Underwater Networks, 2008.

[20] W. Rudin, Principles of Mathematical Analysis, 3rd Edition, McGraw-Hill, 1976.

[21] M. Stojanovic, On the relationship between capacity and distance in an underwater acoustic communication channel, in: Proceedings of the 1st ACM International Workshop on Underwater Networks (WUWNet'06), 2006.

[22] C. Carbonelli, U. Mitra, Cooperative multihop communication for underwater acoustic networks, in: Proceedings of the 1st ACM International Workshop on Underwater Networks (WUWNet'06), 2006.

[23] W. Zhang, U. Mitra, A delay-reliability analysis for multihop underwater acoustic communication, in: Proceedings of the second workshop on Underwater networks (WUWNet '07), ACM, New York, NY, USA, 2007, pp. 57–64.

Appendix

A. Proof of Uniform Convergence

Before proving the theorem, we first state the following facts and prove the subsequent lemmas.

Fact A.1. *Suppose K is compact, and*
(a) $\{f_n\}$ is a sequence of continuous functions on K,
(b) $\{f_n\}$ converges pointwise to a continous function f on K,
(c) $f_n(x) \geq f_{n+1}(x)$ for all $x \in K, n = 1, 2, 3, \ldots$.
Then, $f_n \to f$ uniformly on K.

Reference: Theorem 7.13 in page 150 of [20].

Fact A.2. *If $\{f_n\}$ and $\{g_n\}$ converges uniformly on a set E and they are sequences of bounded functions, then $\{f_n g_n\}$ converges uniformly on E.*

Reference: Page 165 of [20].

Lemma A.1. *Suppose*

$$\begin{aligned} f_n(x) &= \left(1 - \frac{x}{n}\right)^{n-1} \\ f(x) &= e^{-x} \end{aligned}$$

Then the sequence of functions $\{f_n\}, n = 2, 3, \ldots,$ converges uniformly on $x \in [0, 1] \subset \mathcal{R}$ to f.

Proof: Let $X = [0, 1] \subset \mathcal{R}$. From Fact A.1, what we need to show are (i) $f_n(x)$ is continuous on X for all n, (ii) $\{f_n\}$ converges pointwise to a continuous function f on X, (iii) $f_n(x) \geq f_{n+1}(x)$ for all $x \in X, n = 2, 3, 4, \ldots$.

It is easy to see that $f_n(x)$ and $f(x)$ are continuous on X for all n and that $\lim_{n\to\infty} f_n(x) = f(x)$.

Suppose $n \in \{r : r \geq 2, r \in \mathcal{R}\}$. Then,

$$\tilde{f}_n(x) = \frac{\partial f_n(x)}{\partial n} = \left(1 - \frac{x}{n}\right)^{n-1} \left\{ \frac{(n-1)x}{n(n-x)} + \ln\left(1 - \frac{x}{n}\right) \right\}$$

Let

$$g_n(x) = \frac{(n-1)x}{n(n-x)} + \ln\left(1 - \frac{x}{n}\right)$$

Then, $g_n'(x) = \frac{x-1}{(n-x)^2}$. Hence, $g_n(x)$ monotonically decreasing on $[0, 1]$ for all n, which implies that, with the fact that $g_n(0) = 0$, $g_n(x) \leq 0$ for all $x \in [0, 1]$ and all n. Hence, $\tilde{f}_n(x) \leq 0$ for all $x \in X$ and all n implying that $f_n(x)$ is monotonically non-increasing as n increases for all $x \in X$. Therefore, it follows that $f_n(x) \geq f_{n+1}(x)$ for all $x \in X$ and all $n = 2, 3, 4, \ldots$.

□

Theorem A.2. *The integrand of Equation (2) converges uniformly on* $[0,1]$ *if* $p = \frac{\lambda}{n}$ *where* $0 \leq \lambda \leq 1$.

Proof: From Fact A.2, it is sufficient to show that each of terms $\alpha \Pr\{NC|\alpha\}$ with Equations (5) and (6) converges uniformly on its domain of α and it is a sequence of bounded functions on $A = [0,1]$.

First, let us show that the term $(1 - \frac{\lambda}{n} + \frac{\lambda}{n}(\alpha + \beta)^2)^{n-1}$, denoted by $h_n(\alpha)$, converges uniformly on $\alpha \in [0, \beta]$, which is from the case where $0 \leq \alpha \leq \beta \leq 0.5$. Because the range $\Re(\lambda(1-(\alpha+\beta)^2))$ is a compact set in A and $h_n(\alpha)$ can be rewritten as

$$h_n(\alpha) = \left(1 - \frac{\lambda(1-(\alpha+\beta)^2)}{n}\right)^{n-1}$$

its uniform convergence follows from Lemma A.1. And $|h_n(\alpha)| \leq 1$ for all α and all n.

In the similar way, it can be proven that other terms satisfy the conditions without difficulty. Therefore, the claim follows.

□